Nonlinear Calculations of Soft and Hard Beta Limits in NSTX

J. Breslau[1], J. Chen[1], N. Ferraro[2], S. Gerhardt[1], S. C. Jardin[1]
[1]*Princeton Plasma Physics Laboratory, Princeton, NJ, USA*
[2]*General Atomics, San Diego, CA, USA*

It is well known that exceeding the beta limits in a tokamak or ST in some regions of parameter space can lead to a disruption [1,2], whereas in other regions one encounters a "soft limit"[3] where transport is increased locally but the discharge continues. To better understand when the consequences of approaching and then exceeding the beta limit lead to a disruptive thermal quench, we have performed a series of nonlinear simulations of NSTX discharges with different pressure and current profiles as they are heated sufficiently to reach the beta limit.

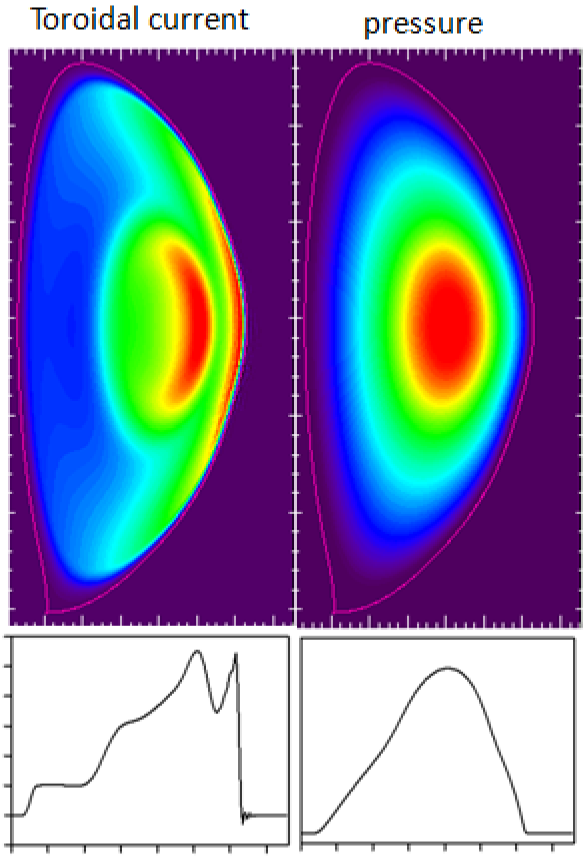

Figure 1: Toroidal current and pressure contours from equilibrium reconstruction of NSTX shot 124379 at time 0.64

We start with the reconstructed equilibrium shown in Figure 1. This came from NSTX shot 124379 at 640 ms. The discharge had $\beta_P \cong 0.8$, $\beta_T \cong 7.3\%$, $q_0 = 1.08$ and a plasma current I_P=1 MA. We used this to initialize a M3D-C^1 calculation with (in code units) resistivity $\eta = 10^{-6}\left(T_0/T\right)^{3/2}$, perpendicular thermal conductivity $\kappa_\perp = 1.2\times10^{-6}(T_0/T)^{1/2}$, viscosity $\mu = 10^{-6}$, and parallel thermal conductivity $\kappa_\| = 10$ with only Ohmic heating, and with a controller to apply a loop voltage to keep the plasma current constant in time. The β vs. time is shown in Figure 2 for both a 3D and a 2D calculation with identical transport coefficients.

Figure 3 shows the Poincare plots of the magnetic field and the incremental change in the electron temperature (from the start of the calculation) at four different times in the 3D calculation. It can be seen that the surfaces initially deform, then become stochastic in the center, but eventually completely heal and the configuration returns to axisymmetry to a high degree by the final time t=6000.

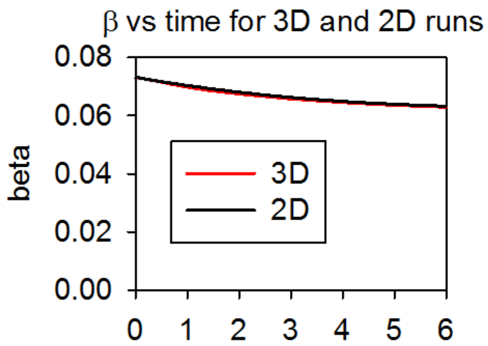

Figure 2: Plasma β vs time for 2D and 3D simulations with same transport coefficients.

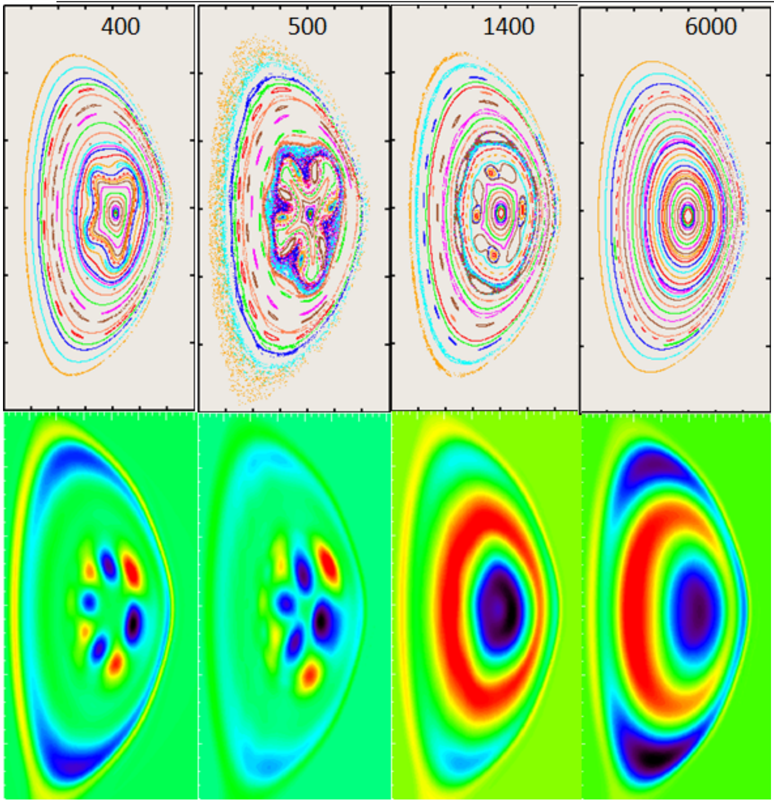

Figure 3: Poincare plots (top) and change in temperature (bottom) from the start of the calculation at 4 different times.

The temperature snapshots in Figure 3 show that initially a single mode grows up (n=3, m=4), and then nonlinearly couples to other modes, and finally the temperature resymmetrizes and becomes constant on flux surfaces. (Note that because of the change in the shift of the magnetic axis, the final temperature snapshot shows in-out distortion).

Figure 4 shows midplane profiles of the electron temperature at the final time for both the 2D and the 3D calculations. It is seen that the result of the 3D instability was to lower the temperature in the center, and to slightly raise the temperature at mid-radius, such that the integral of the thermal energy (as measured by β) stays unchanged from the 2D calculation. The net effect of the localized 3D MHD instability was to increase the effective thermal transport in the center of the discharge. This is an example of a soft β-limit.

We next repeat this calculation but include a neutral beam energy and momentum source so that the plasma β remains approximately constant in time. The strength of the beam energy source is chosen so that the plasma beta remains constant in time for the T=5000 τ_A duration of the initial run, using the same transport model as discussed previously, except that the plasma viscosity is increased to $\mu = 10^{-4}$ so that the maximum rotation velocity is about 0.02 V_A. This now causes the magnetic surfaces to distort, as can be seen in the Poincare plot marked "1" in Figure 5.

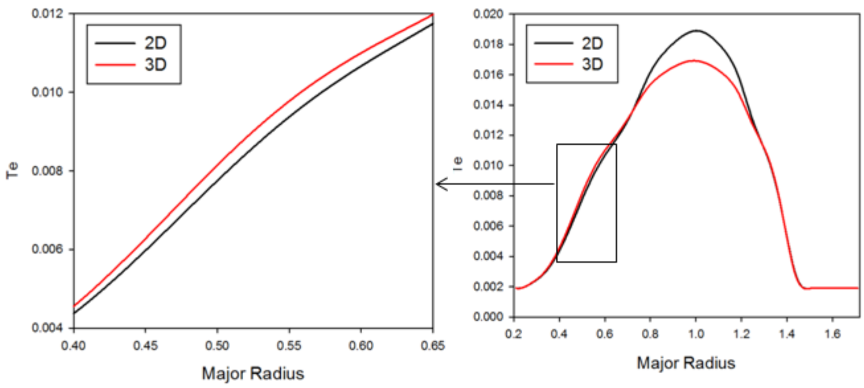

Figure 4: Midplane temperature profiles in the 3D and the 2D calculations. The net effect of the 3D instability was to transport some energy out from the plasma center to the mid-radius position.

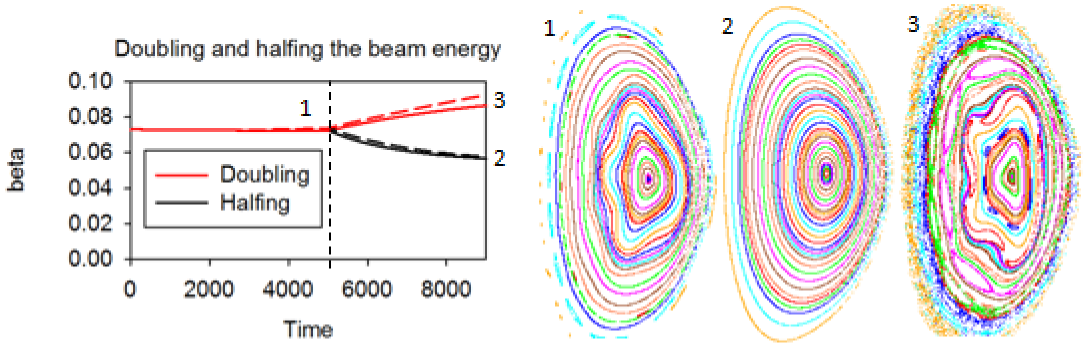

Figure 5: Poincare plots of the magnetic surfaces "1" at T=5000 τ_A, and at T=9000 τ_A with "2" the neutral beam power halved, and "3" the neutral beam power doubled. Dashed curves are 2D calculations with same transport coefficients.

Next, we restarted these runs at T=5000 τ_A with (2) the beam power halved, and (3) the beam power doubled. (What was actually done in the code was to keep the beam power and torque fixed, but to (2) double and (3) half the perpendicular thermal conductivity, producing the same effect but keeping the sheared toroidal velocity constant.) We see that in case (2), with the beam power effectively halved, the surfaces again become regular and axisymmetric. In case (3), with the beam power effectively doubled, the surfaces become severely deformed with islands and stochastic regions.

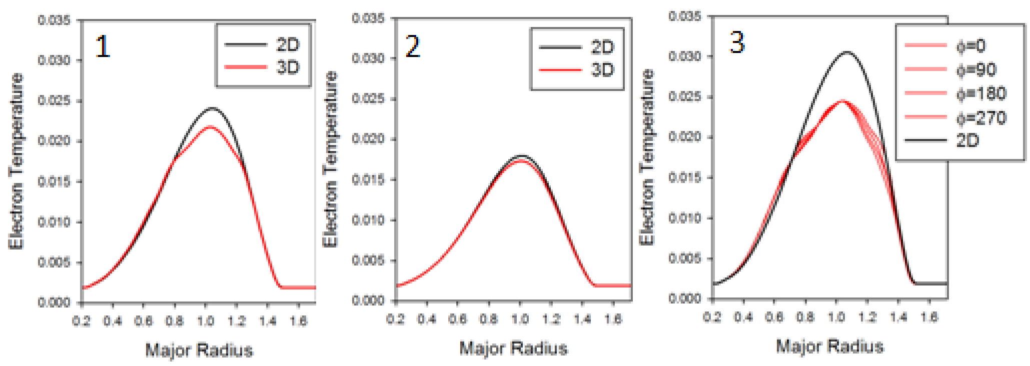

Figure 6: Midplane temperature profiles for the three time points in Figure 5 for both the 3D and 2D calculations with the same transport coefficients.

The midplane profiles of the temperature for both 2D and 3D are shown in Figure 6, and the toroidal harmonics vs. time of the kinetic energy for the two cases shown in Figure 5 are shown in Figure 7.

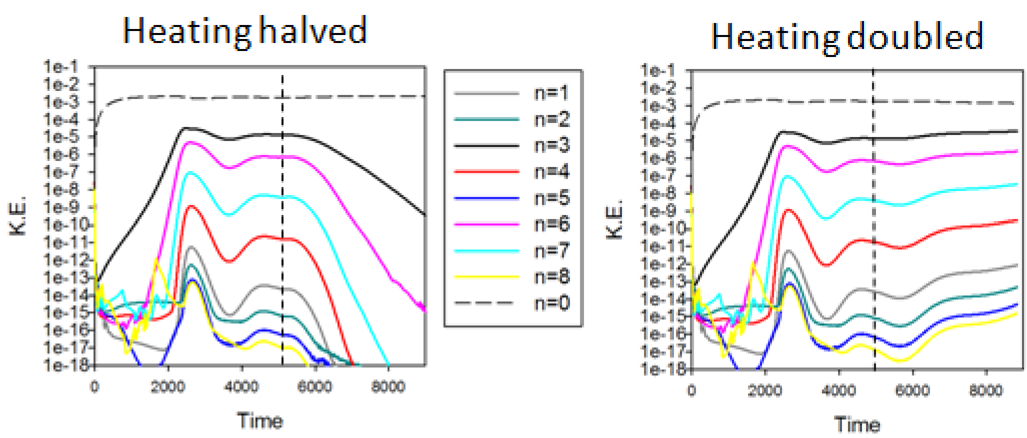

Figure 7. Kinetic energy of each velocity toroidal harmonic for the 2 3D cases shown in Figure 5.

The time dependence of the case shown in Figures 1-4 is to be contrasted with that shown in Figure 8, which is for the identical equilibrium current and pressure profiles but with the toroidal field scaled at the edge to be 0.8 times its original value (Bateman scaled). This resulted in an equilibrium with β=10.6%. q_0 = 1.08. This is seen to be linearly unstable to many modes, and to produce stochastic flux surfaces over most of the cross section (rightmost plots are at the final time T=3750) so that the 2D and 3D calculations give markedly different results.

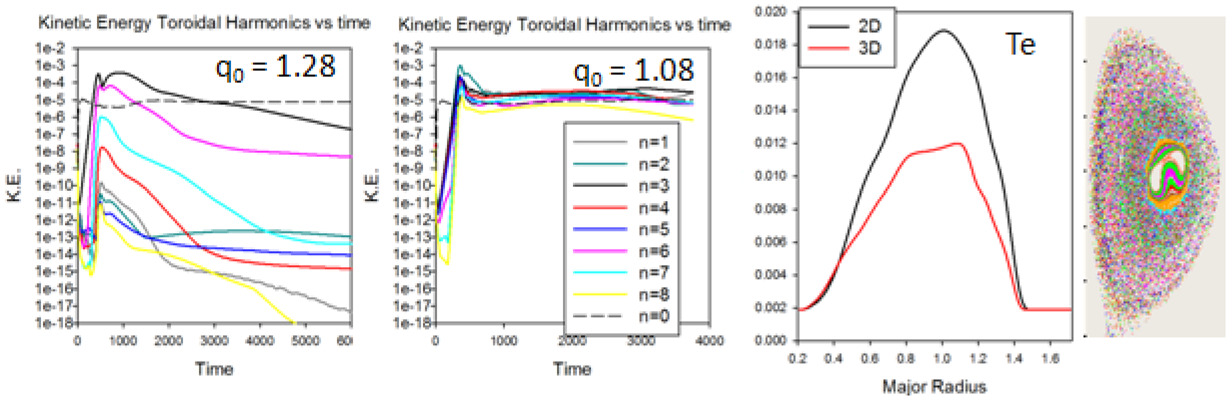

Figure 8: Leftmost plot shows harmonics of kinetic energy starting with the equilibrium studied in Figures 1-4. The three plots on the right are for the time dependence of that equilibrium Bateman scaled by a factor of 0.8.

In conclusion, we observe that if, as β is increased, only a single mode first becomes unstable, such as with the q_0=1.28 equilibrium, the surfaces can distort and may exhibit local stochasticity to relax the local pressure gradients, but can recover if the beta is lowered. In contrast, if many modes are unstable such as in the q_0=1.08 equilibrium, a large volume can become stochastic and this can lead to a thermal collapse and subsequent disruption. Future studies will qualify this observation by extending the range of equilibrium and heating scenarios examined.

Acknowledgments:

This project has benefited greatly from software developed and provided by M. Shephard and the SCOREC team at Rensselaer Polytechnic Institute. This work was supported by the US DOE contract no. DEAC02-09CH11466 and the SciDAC Center for Extended Magnetohydrodynamic Modeling.

References:

[1] W. Park, E. Fredrickson, A. Janos, et al, "High-beta disruption in tokamaks", Phys Rev. Lett. **75** 1763-1766 (1995)

[2] S. Kruger, D. Schnack, et.al., "Dynamics of the major disruption of a DIII-D plasma", Phys. Plasmas **12**, 056113 (2005)

[3] O. Sauter, R. LaHaye, Z. Chang, et al, "Beta limits in long-pulse tokamak discharges", Phys. Plasmas **4** 1654 (1997)

[4] S. Jardin, N. Ferraro, J. Breslau, J. Chen, "Multiple timescale calculations of sawteeth and other global macroscopic dynamics of tokamak plasmas", Computational Science and Discovery (2012) **5** 014002

[5] J. Breslau, M. Chance, J. Chen, et al, "Onset and saturation of a non-resonant internal mode in NSTX and implications for AT modes in ITER", Nucl. Fusion **51** (2011) 063027

[6] S. P. Gerhardt, et al., "Disruptions, disruptivity, and safer operating windows in the high-β spherical torus NSTX", submitted to Nuclear Fusion (2012)

[7] G. Bateman and Y.K. M. Peng, "Magnetohydrodynamic stability of flux-conserving tokamak equilibria" Phys. Rev. Lett. **38** 829-831 (1977)